BMC Cancer

RESEARCH Open Access

Identifying high-risk candidates for prolonging progression-free survival in primary gastric carcinoma subject to "double invasion": an analytical approach utilizing lasso-cox regression

Liwei Wang[1], Yu Chang[1], Jinfeng Ma[1], Wenqing Qu[1*] and Yifan Li[1*]

Abstract

Objective To identify high-risk gastric carcinoma patients with concurrent vascular and neural invasion ("double invasion") who are at heightened risk of progression-free survival (PFS) decline, enabling personalized clinical management.

Methods In this multi-center retrospective study, 559 patients with double invasion who underwent curative gastrectomy between May 2002 and December 2020 were analyzed. Prognostic factors for PFS were identified using Lasso-Cox regression. Model validation included internal bootstrapping, calibration plots, and comparison against the American Joint Committee on Cancer(AJCC) 8th edition TNM staging system via Harrell's C-index, decision curve analysis (DCA), and time-dependent receiver operating characteristic (ROC) curves.

Results The nomogram integrated gender, positive lymph node count, surgical gastrectomy method, PTEN/FHIT expression levels, and maximum tumor diameter. It demonstrated superior predictive accuracy to AJCC staging, with a C-index of 0.651 (95% CI: 0.612–0.691) versus 0.543 (95% CI: 0.517–0.569). Calibration plots showed strong agreement between predicted and observed outcomes. The area under the curve(AUC) for 3- and 5-year PFS predictions were 0.719 (95% CI: 0.655–0.771) and 0.767 (95% CI: 0.670–0.841), respectively. DCA confirmed clinical utility across decision thresholds, and risk stratification effectively differentiated low- and high-risk groups. In the training cohort, the model significantly outperformed AJCC staging (NRI: 0.218, $p < 0.01$; IDI: 0.085, $p < 0.01$). However, this superiority was not statistically significant in the validation cohort (NRI: 0.141, $p = 0.08$; IDI: 0.031, $p = 0.239$).

Conclusion We developed a Lasso-Cox regression-based nomogram to stratify PFS risk in gastric carcinoma patients with double invasion. While the model outperformed AJCC staging in training, validation cohort results highlight

*Correspondence:
Wenqing Qu
18536669539@qq.com
Yifan Li
lyf8028@126.com

Full list of author information is available at the end of the article

the need for further refinement. This tool holds potential for guiding tailored therapeutic strategies, though broader validation is warranted to confirm clinical applicability.

Keywords Gastric cancer, Progression-free survival, Nomogram, Risk stratification, Vascular invasion and neural invasion

Introduction

Gastric cancer, ranking as the fifth most commonly diagnosed malignancy and the fourth leading cause of cancer-related deaths globally, continues to command critical attention in worldwide health circles [1]. Yet, the emergence of advanced medical technologies has engendered several effective treatments, such as endoscopy, surgery, radiation, chemotherapy, and immunotherapy, substantially improving the prognostic landscape for those afflicted with this disease [2–6]. Central to these interventions is the radical surgical excision of the tumor, a procedure that stands as the cornerstone of treatment for patients with operable, non-metastatic gastric cancer [7–8], significantly influencing survival rates [9–11].

A pivotal element evaluated in most gastric cancer staging systems is the extent of vascular and neural infiltration, a crucial factor that independently predicts recurrence-free survival following R0 resection. Our retrospective study revealed that patients with concurrent vascular and neural invasion have an average overall survival of 34.49 ± 24.02 months and an average progression-free survival of 27.58 ± 21.15 months, highlighting the prognostic significance of this "double invasion" phenomenon. Nevertheless, reliably forecasting the progression of gastric cancer in the presence of "double invasion" presents a significant clinical challenge. In response to this urgent need for improved prognostic accuracy, our research employs advanced methodologies to develop predictive models specifically designed for patients with "double invasion." Our findings emphasize the importance of considering this dual-invasive pattern during the prognostic evaluation of gastric carcinoma. Our main goal was to refine a prognostic nomogram capable of accurately predicting outcomes for gastric carcinoma patients, particularly those experiencing concurrent vascular and neural invasion. Additionally, we included a risk stratification framework to distinguish among patients who may benefit from chemotherapy, those at risk of overtreatment, and those who could gain from a multidisciplinary therapeutic approach. By adopting the precision medicine paradigm, these nomograms and risk stratification strategies offer tailored guidance for postoperative management of gastric carcinoma, paving the way for more personalized and effective treatment pathways for individual patients.

Method

Data collection

In Shanxi Province, a thorough investigation was initiated. It examined the medical records of 1,650 patients who underwent gastrectomy for gastric cancer at three leading medical institutions: Shanxi Cancer Hospital, Yuanqu County People's Hospital, and Hongtong County People's Hospital. This investigation spanned from May 2005 to December 2022. Among these patients, 559 were diagnosed with gastric carcinoma displaying dual invasiveness; these individuals were meticulously randomized into a training cohort of 388 and a validation cohort of 171.

The inclusion criteria for this scholarly endeavor required a confirmed diagnosis of gastric adenocarcinoma, unrestricted access to clinicopathological details and follow-up records, no severe postoperative organ dysfunction, and a medical history lacking prior unrelated cancers or causes of mortality. Those affected by systemic malignancies, incomplete datasets, palliative surgeries, or cancers not originating in the stomach were excluded. Tumor staging strictly followed the AJCC 8th TNM classification system. The Shanxi Cancer Hospital Ethics Committee provided the study's ethical foundation. All participants provided informed consent, and patient confidentiality was diligently maintained throughout. Figure 1 presents a detailed research process flowchart, while Fig. 2 offers an overview of the methodology. The essential criterion for participation in this study was histologically confirmed gastric cancer, along with a history of curative surgery with negative margins. The research team thoroughly evaluated various factors that could influence surgical outcomes, including, but not limited to, the patient's gender, age at the time of surgery, the extent of tumor invasion into blood vessels and nerves, tumor progression, the number of lymph nodes affected by the malignancy, the Lauren classification, the size of cancer, the type of gastrectomy performed, and the expression of several biomarkers (AE1/AE3, CK20, CDX-2, SATB-2, SYN, CGA, CD56, PTEN, PHIT, MLH1, PMS2, Her-2, MSH2, and MSH6), as well as the length of progression-free survival. The study's timeframe was established through a detailed review of the patient's medical records, consultations with oncological specialists, and tracking the most recent hospital visit until the final engagement with the surgical team. Progression-free survival was defined as the interval from the surgical intervention to the patient's death or disease progression.

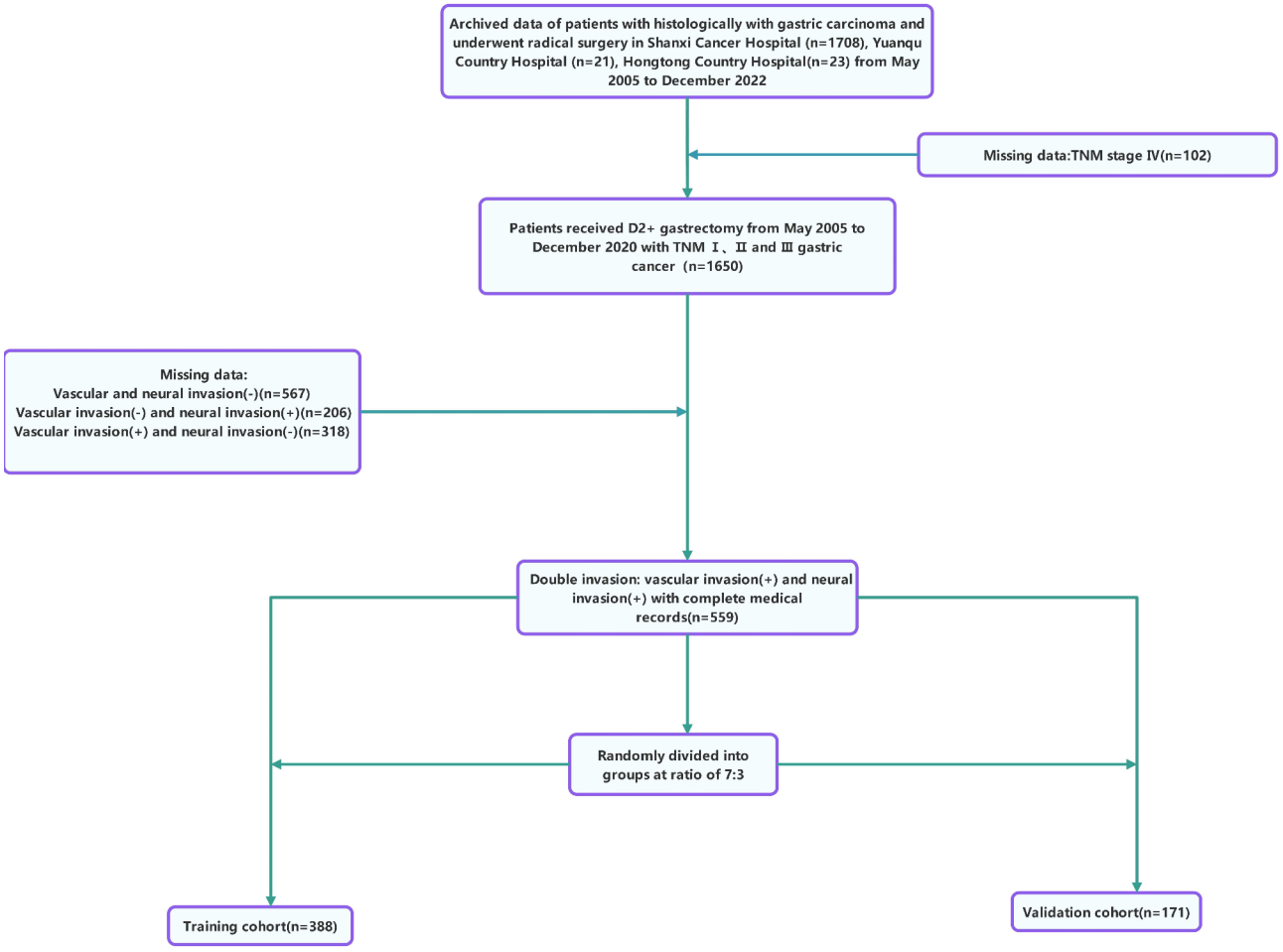

Fig. 1 The flowchart of study population enrollment in the training and validation cohort of gastric cancer illustrates the sequential process of participant selection for the research study. Initially, a pool of potential candidates with gastric cancer is identified. Subsequently, individuals are excluded based on specific criteria, such as the presence of other concurrent cancers, refusal to participate, or incomplete medical records. The remaining participants are randomly assigned to either the training or validation cohort. The training cohort is used to develop the predictive models, while the validation cohort tests and validates the performance of these models independently

In addressing the issue of missing data, we adopted a dual strategy: values absent in more than 30% of the variables were excised from the dataset, whereas those with less than 30% missingness were imputed by substituting the mean of their respective variables. This scholarly inquiry conducted a retrospective analysis of clinical data, carefully gathered in compliance with institutional protocols and regulatory standards, obtaining all participants' informed consent following the Declaration of Helsinki guidelines, thus linking scientific rigor with ethical integrity.

Statistical analysis

To achieve a nuanced statistical portrayal of our dataset, we conducted a descriptive statistical analysis to distill its essence into a comprehensive summary. Categorical variables were presented in discrete forms, while continuous variables were summarized through their medians and interquartile ranges, outlining their intrinsic characteristics. The Kaplan-Meier curve was our chosen method for a graphical representation of progression-free survival (PFS), which is well-known for effectively illustrating survival trends. We applied Lasso-Coxregression analyses to explore the relationship between PFS and various factors. These analytical strategies allowed us to convey our insights using hazard ratios, 95% confidence intervals (CIs), and p-values, thus providing a solid foundation for evaluating statistical significance. A p-value less than 0.05 was considered indicative of statistical significance. Our statistical computations were performed with precision using various software tools, including R version 4.3.2, developed by The University of Auckland, Auckland, New Zealand, and SPSS version 25.0, created by IBM Corp., Armonk, NY, USA, ensuring the seamless application of our statistical rigor.

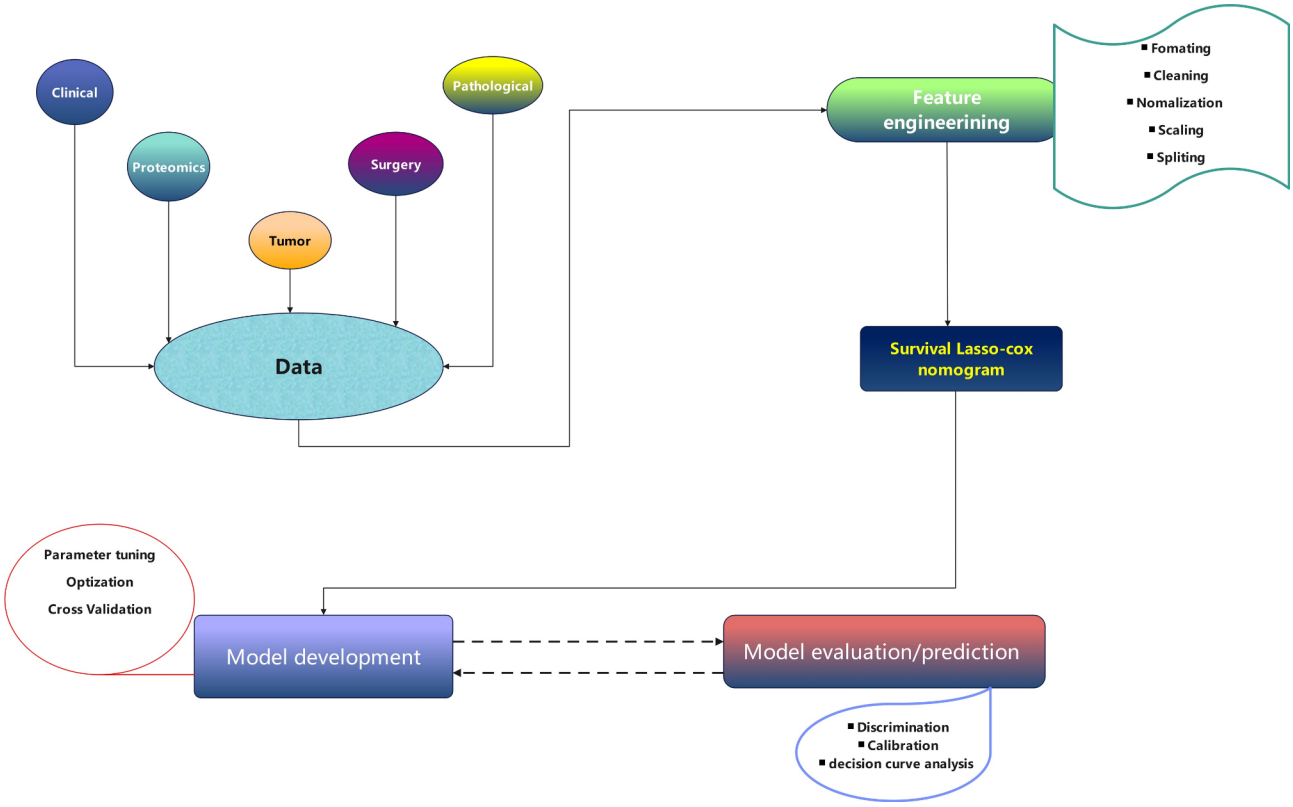

Fig. 2 presents the data management workflow and develops a prediction model for gastric cancer progression-free survival (PFS). The workflow begins with collecting and preprocessing patient data, including demographic information, clinical characteristics, and molecular data. The collected data is then curated and formatted to ensure consistency and accuracy before it is split into the training and validation datasets. The subsequent steps involve feature selection and the implementation of machine learning algorithms to develop the PFS prediction model. After creating the model, it undergoes internal validation using cross-validation techniques and external validation with a separate dataset

Nomogram performance

This investigation aimed to refine demographic tools for predicting progression-free survival (PFS) by amalgamating variables identified through Lasso-Cox regression analyses. It was anchored in a robust validation framework characterized by 10,000 iterative cycles for internal validation and an external validation phase using a distinct patient cohort. Risk determinants were carefully identified and stratified according to clinical benchmarks or tertiles, forming the basis of the prediabetes score model. These categorical risk factors were incorporated into a systematic stepwise Cox proportional hazards regression, resulting in a novel set of β coefficients. The scoring mechanism was developed by tripling the regression coefficients and rounding to the nearest integer to assign numerical scores. These scores were then transformed into a user-friendly questionnaire suitable for primary care professionals. Patients were subsequently divided into low and high-risk cohorts based on cumulative scores. The model's predictive accuracy for PFS in gastric cancer patients, including those with lymphatic metastasis, was rigorously evaluated. Survival probabilities and time-to-event metrics were measured using the Kaplan-Meier technique, with the log-rank test employed to assess differences in PFS between risk categories. The model's discriminative ability was evaluated through calibration and discrimination metrics, such as Harrell's C-Index and the area under the ROC curve (AUC). An AUC ranging from 0.5 to 0.7 indicates suboptimal discrimination; scores between 0.7 and 0.9 signify moderate discriminative ability, while an AUC exceeding 0.9 represents exceptional performance [12, 13]. The consistency of the results was confirmed through calibration plots, and the clinical utility of the nomograms was examined using decision curve analysis (DCA) [14–16].

Results

Essential characteristics of training cohort and validation cohort of double invasion

In the training cohort, we included 388 gastric cancer patients with double invasion and 171 with double invasion in the validation cohort; each variable was balanced in the two groups(Table 1).

Table 1 Demographics of study population

Variables	Double invasion ($n=388$) Training cohort	Double invasion ($n=171$) Validation cohort	*P*
	Mean ± SD/No(%)	Mean ± SD/No(%)	
Gender			0.258
Male	321(82.7%)	148(86.5%)	
Female	67(17.3%)	23(13.5%)	
Age (years)	58.94 ± 10.11	58.81 ± 9.74	0.683
pT stage			0.801
T1	4(1.0%)	1(0.6%)	
T2	5(1.3%)	1(0.6%)	
T3	112(28.9%)	47(27.5%)	
T4	267(68.8%)	122(71.3%)	
Number of positive lymph nodes			0.654
0	35(9.0%)	10(5.8%)	
1–2	60(15.5%)	27(15.8%)	
3–6	71(18.3%)	33(19.3%)	
≥ 7	222(57.2%)	101(59.1%)	
pTNM stage			0.176
I	5(1.3%)	0	
II	61(15.7%)	21(12.3%)	
III	322(83.0%)	150(87.7%)	
Lauren classification			0.471
Intestinal	60(15.5%)	21(12.3%)	
Diffuse	238(61.3%)	104(60.8%)	
Mixed	90(23.2%)	46(26.9%)	
Type of gastrectomy			0.779
Proximal	23(5.9%)	8(4.7%)	
Distal	84(21.6%)	40(23.4%)	
Total	152(39.4%)	123(71.9%)	
PTEN			0.653
Negative	309(79.6%)	139(81.2%)	
Positive	79(20.4%)	32(18.8%)	
FHIT			0.667
Negative	321(82.7%)	144(84.2%)	
Positive	67(17.3%)	27(15.8%)	
Her-2			0.715
Negative	232(59.8%)	103(60.2%)	
Positive	156(40.2%)	68(39.8%)	
AE1/AE3			0.958
Negative	30(7.7%)	13(7.6%)	
Positive	358(92.3%)	158(92.4%)	
Ki167(%)	67.93 ± 18.85	69.56 ± 18.86	0.289
CK7			0.339
Negative	194(50.0%)	93(54.4%)	
Positive	194(50.0%)	78(45.6%)	
CK20			0.826
Negative	287(74.0%)	128(74.9%)	
Positive	101(26.0%)	43(25.1%)	
CDX-2			0.634
Negative	198(51.0%)	91(53.2%)	
Positive	190(49.0%)	80(46.8%)	
SATB-2			0.852
Negative	309(87.3%)	135(78.9%)	
Positive	79(12.7%)	36(21.1%)	

Table 1 (continued)

Variables	Double invasion (*n* = 388) Training cohort	Double invasion (*n* = 171) Validation cohort	*P*
	Mean ± SD/No(%)	Mean ± SD/No(%)	
SYN			0.767
Negative	272(70.1%)	122(71.3%)	
Positive	116(29.9%)	49(28.7%)	
CGA			0.721
Negative	332(83.0%)	144(84.2%)	
Positive	66(17.0%)	27(15.8%)	
CD56			0.625
Negative	232(59.8%)	468(60.2%)	
Positive	156(40.2%)	310(39.8%)	
MLH1			0.801
Negative	25(6.4%)	12(7.0%)	
Positive	363(93.6%)	159(93.0%)	
PMS2			0.712
Negative	72(18.6%)	34(19.9%)	
Positive	316(81.4%)	137(80.1%)	
MSH2			0.458
Negative	21(5.4%)	12(7.0%)	
Positive	367(94.6%)	159(93.0%)	
MSH6			0.855
Negative	19(4.9%)	9(5.3%)	
Positive	369(95.1%)	162(94.7%)	
Maximum diameter of Tumor(cm)	5.92 ± 2.51	5.92 ± 2.37	0.893
Tumor location			0.656
Upper 1/3	224(57.7%)	95(55.6%)	
Middle 1/3	74(19.1%)	29(17.0%)	
Lower 1/3	88(22.7%)	46(26.9%)	
Multiple	2(0.5%)	1(0.6%)	

Abbreviations: SD, standard deviation; No, number

Development and validation of the prediction model of PFS for double invasion

In meticulously examining the natural history underlying gastric cancer with biphasic invasive characteristics, we employed Lasso-Cox regression analysis to identify the key variables predicting progression-free survival (PFS). This analytical process filtered out most covariate coefficients, leaving six parameters that emerged as strong, independent prognostic markers (cf. Figure 3). These essential factors included patient sex, the number of positive lymph nodes, the surgical approach to gastrectomy, the molecular biomarker expressions of PTEN and FHIT, and the tumor's maximum diameter. These parameters were vital in creating a nomogram, a predictive tool designed to estimate the 3-year and 5-year PFS probabilities for patients with gastric cancer exhibiting dual invasive pathways (illustrated in Fig. 4 and Table 2). Notably, this prognostic tool effectively identified patients with a more favorable outlook. In the training cohort, the nomogram achieved a C-index of 0.651 (95% confidence interval(CI): 0.612–0.691) for PFS prediction, surpassing the discriminative power of the 8th edition of the AJCC-TNM staging system, which recorded a C-index of 0.543 (95% CI: 0.517–0.569). This difference highlights the superior predictive accuracy of our nomogram.

Based on Lasso-Cox regression, the nomogram was thoroughly validated for predictive accuracy through rigorous internal validation, utilizing 1,000 bootstrap resamples from the training cohort and external validation on a distinct dataset. Figure 5A and D show that the calibration plots illustrate a strong concordance between the nomogram's predictions and actual outcomes, thereby validating its prognostic accuracy. Furthermore, during internal validation, the nomogram's discriminative ability to distinguish between different prognostic outcomes was confirmed through time-dependent receiver operating characteristic (t-ROC) curve analyses. Specifically, for 3-year PFS, the nomogram produced an area under the curve (AUC) of 0.719, with a 95% confidence interval (CI) ranging from 0.655 to 0.771 for internal validation and 0.647 (95% CI: 0.558–0.754) for external validation. For 5-year PFS, the AUC was 0.767 (95% CI: 0.670–0.841) for internal validation and 0.718 (95% CI: 0.528–0.820) for external validation, as depicted in Fig. 6A and B. Decision

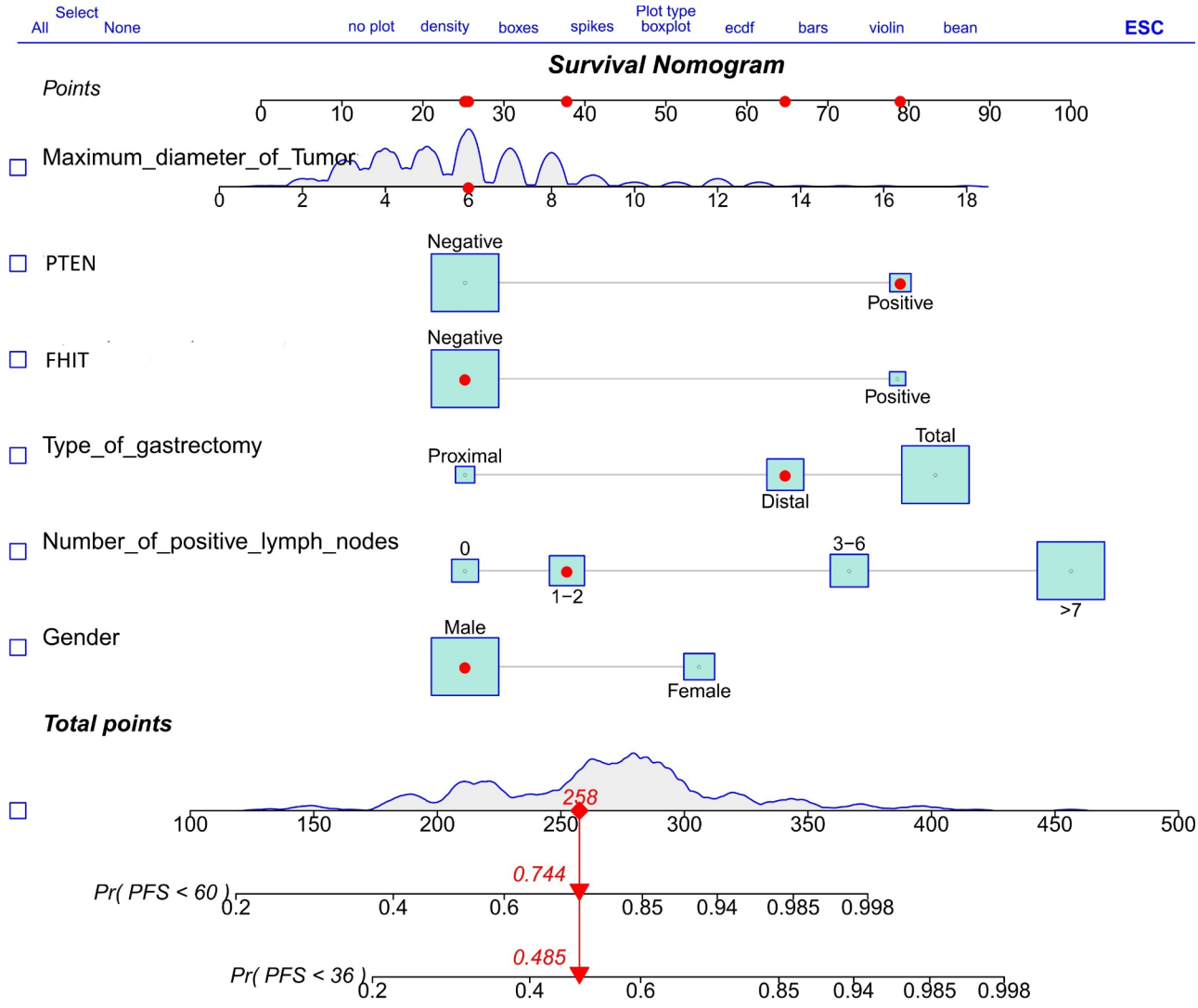

Fig. 3 As depicted in Fig. 3, the nomogram model is a graphical tool designed to predict the 3-year and 5-year PFS probabilities of patients with gastric cancer. The model is based on the results of Lasso-cox regression analysis, which identifies the most significant predictors of PFS. The nomogram incorporates these predictors into a user-friendly, point-based system, where each predictor is assigned a certain number of points corresponding to its contribution to the risk of PFS. By summing the points for each predictor and locating the total on the nomogram scale, clinicians can estimate a patient's PFS probability, thus aiding in treatment planning and patient counseling

Curve Analysis (DCA) was conducted to compare its 3-year and 5-year PFS predictions against those of the AJCC 8th edition TNM staging system to evaluate the nomogram's clinical utility. The nomogram achieved a C-index of 0.651 (95% CI: 0.612–0.691) in internal validation and 0.615 (95% CI: 0.552–0.677) in external validation, as illustrated in Fig. 7A and D. These C-index values demonstrate the superior predictive performance of the nomogram compared to the established AJCC staging system. Moreover, the Lasso-cox model showed a marked enhancement in predictive accuracy for the 8th AJCC TNM classification relative to the conventional 8th AJCC TNM staging, as reflected by a notable Net Reclassification Index (NRI) of 0.218 ($p < 0.01$) and an Incremental Discrimination Index (IDI) of 0.085 ($p < 0.01$) within the training cohort. Despite these improvements, the nomogram's predictive edge over the established AJCC staging system was not discernible within the validation cohort, as indicated by an NRI of 0.141 ($p = 0.08$) and an IDI of 0.031 ($p = 0.239$). (Table 3).

Risk scoring of stratification system of PFS for double invasion

The refined Lasso-Cox regression-based nomogram model assigned a personalized risk score for each patient, aiding in their classification. By establishing a threshold of 137.26, we divided the 559 patients into two distinct groups, each exhibiting different propensities for disease progression, as shown in Fig. 8A and B, and 8C. The low-risk group consisted of 120 individuals from the training

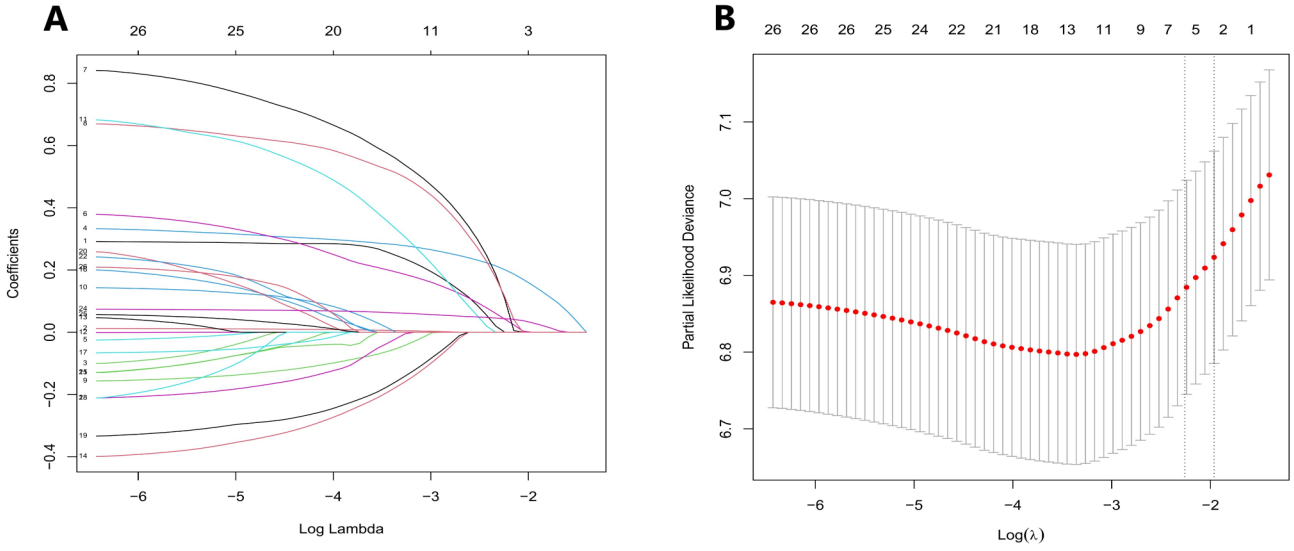

Fig. 4 **(A)** The LASSO coefficient profiles in Fig. 4 A represent a graphical summary of the selection process for the variables that contribute to predicting progression-free survival (PFS) in patients with "double invasion" gastric cancer. As the log lambda regularization parameter varies, the coefficients of the 29 variables included in the model change, with some variables being progressively eliminated due to their non-significant contribution to the model's predictive power. The profile provides insights into the most influential factors that affect PFS in this subset of gastric cancer patients. **(B)** The relationship between the log lambda and the mean-squared error (MSE) in the LASSO regression, as shown in Fig. 4 B, highlights the trade-off between model complexity and prediction accuracy. As the log lambda increases, the model complexity decreases as less essential variables are excluded. Concurrently, the MSE initially decreases, indicating improved model performance, but may eventually start to increase if too many relevant variables are excluded, leading to underfitting. This plot helps select the optimal regularization parameter that balances the model's predictive performance with its interpretability

Table 2 Multivariate analysis of PFS of training cohort of double invasion and analyzed by Lasso-cox regression

	B	SE	Wald	df	*p*	Exp(B)	EXP(95%CI)
Type of gastrectomy			6.643	2	0.033		
Proximal Vs. Distal	0.73	0.543	1.81	1	0.179	2.076	0.697–5.831
Proximal Vs. Total	0.895	0.407	4.84	1	0.028	2.431	1.102–5.364
PTEN				1			
Negative Vs. Positive	0.708	0.242	8.598	1	0.003	2.031	1.265–3.261
FHIT				1			
Negative Vs. Positive	0.927	0.283	10.77	1	0.001	2.528	1.453–4.398
CK20				1			
Negative Vs. Positive	-0.418	0.171	6.001	1	0.014	0.658	0.471–0.920
CD56				1			
Negative Vs. Positive	-0.345	0.166	4.314	1	0.038	0.708	0.511–0.981
Maximum diameter of Tumor	0.076	0.028	7.323	1	0.007	1.079	1.021–1.140

Abbreviations: B, regression coefficient; SE, standard error; *df*, degree of freedom; HR, hazard ratio; CI, confidence interval

set ($n = 388$) and 53 from the validation set ($n = 171$), whose risk scores did not exceed the 137.26 cutoff. In contrast, the high-risk group included 268 patients from the training set and 118 from the validation set, all with scores surpassing this threshold. Figure 9C and D, and 9E present the survival curves for the entire cohort and the training and validation subsets, illustrating a clear stratification according to risk score with P values below 0.001. The median progression-free survival (PFS) for the low-risk group was 61 months for the entire cohort, 77 months for the training subset, and 48 months for the validation subset. The median PFS for the high-risk group was consistently 24 months across all three subsets. The marked difference in survival outcomes between these two risk groups highlights the effectiveness of our model in stratifying patient risk.

Figure 9A illustrates the relationship between risk score and progression-free survival (PFS) in the training cohort, showing a noticeable decline in the 3-year PFS rate as risk scores increase, particularly evident beyond a score of 100 (ranging from 58.6% for the 100–150 group to 15.3% for the 200–363 group). The trend for the 5-year PFS rate demonstrates an even sharper decrease, starting at 81.8% in the lowest risk score group (0–50) and dropping to 12.3% in the highest group (200–363). Figure 9B further emphasizes the connection between risk

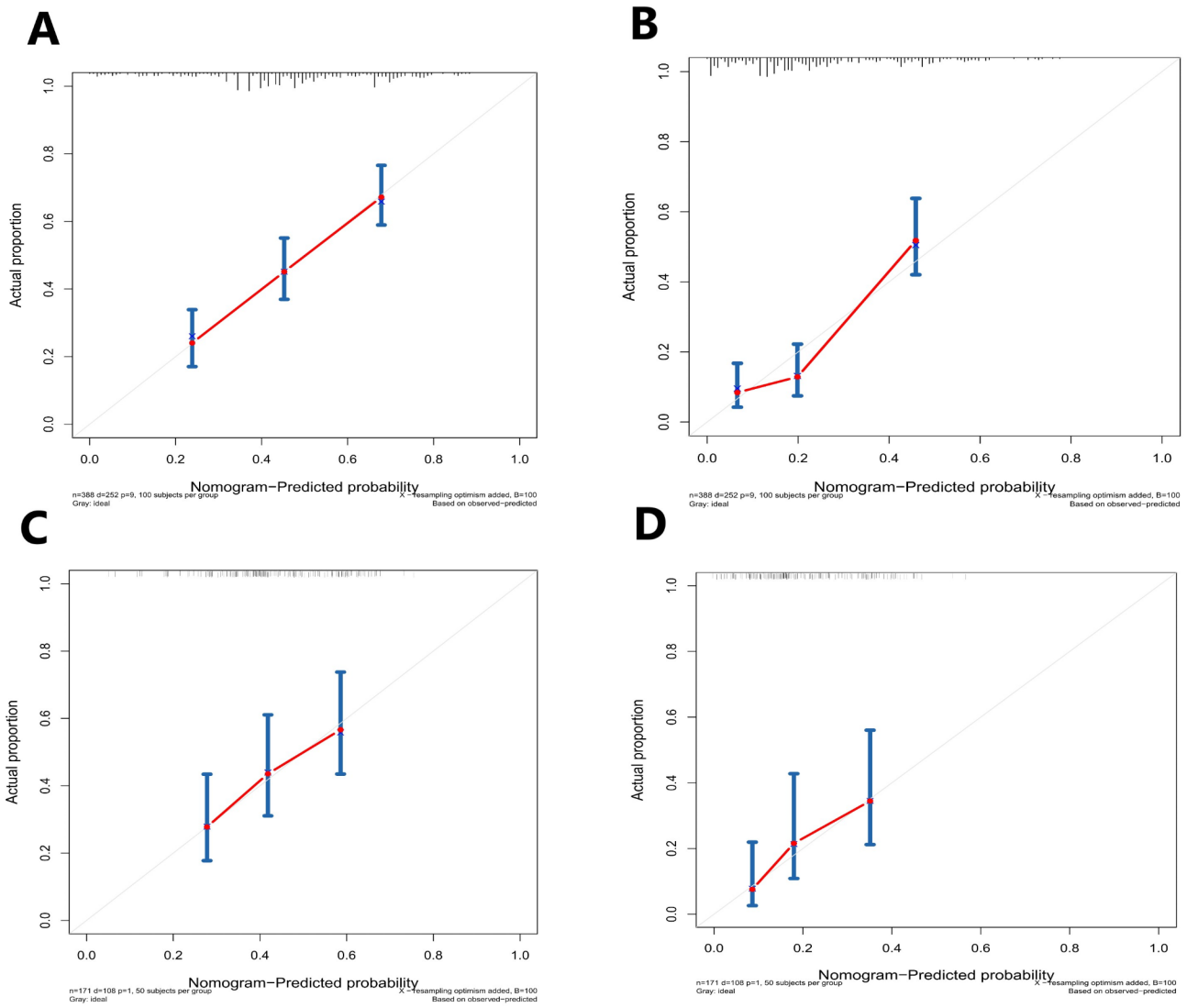

Fig. 5 Calibration curves are shown here to illustrate the predictive accuracy of the Lasso-Cox regression model for the 3-year and 5-year PFS of patients with "double invasion." **(A)** This subfigure presents the internal validation results for the 3-year PFS predictions the Lasso-Cox regression model made. The calibration curve compares predicted probabilities with observed outcomes, assessing the model's accuracy. **(B)** This subfigure displays the external validation results for the 3-year PFS predictions. Like the internal validation, the calibration curve here evaluates how well the model predicts actual patient outcomes in an independent dataset. **(C)** This section focuses on the internal validation of the 5-year PFS predictions. The calibration curve assesses the model's predictive accuracy over an extended period. **(D)** The external validation for the 5-year PFS predictions is highlighted in this subfigure, where the model's predictions are compared to the observed survival data in an external cohort to validate its generalizability

score and PFS rate, revealing a consistent reduction in 5-year survival probability as risk scores rise. This decline is evident from the start, with survival rates decreasing to 56.5% for the 100–150 group, 17.9% for the 180–200 group, and 17.2% for the 200–314 group. Similarly, the 3-year survival rate follows this pattern, falling from 56.5% in the lowest risk category (0–50) to 24.1% in the 200–314 range. These graphical representations confirm the strong link between risk score and survival outcomes, supporting our risk stratification model for PFS prediction. They also highlight the prognostic significance of risk assessment in predicting survival within the scope of this study.

Discussion

Vascular invasion, where gastric cancer cells infiltrate blood vessels beyond the muscularis propria, is a critical hallmark of the disease, as documented in reference [17]. This infiltration mode significantly influences the most effective therapeutic approach and predicts the clinical trajectory for patients with gastric cancer. Its prognostic importance is further heightened by its classification as a key determinant of patient prognosis. The intricate

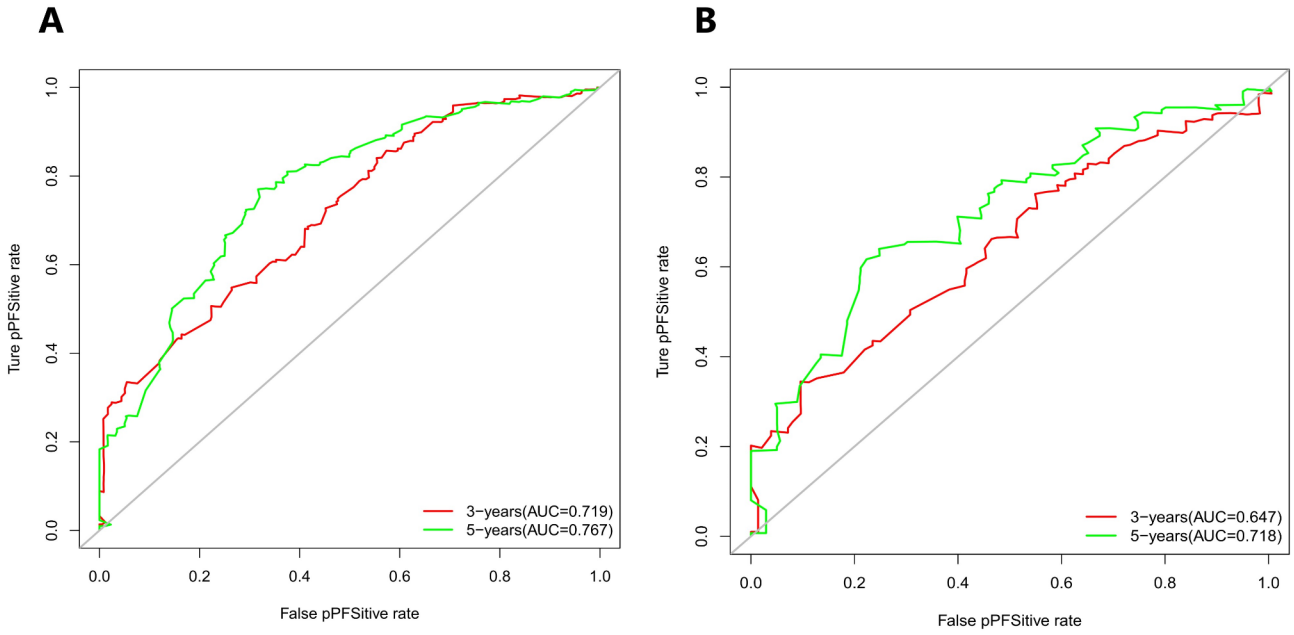

Fig. 6 Time-dependent receiver operating characteristic (t-ROC) curves are used to assess the performance of the Lasso-Cox regression model in predicting PFS for patients with "double invasion" over time. **(A)** This subfigure demonstrates the internal validation of the Lasso-Cox regression model's predictive capability, illustrating how effectively it differentiates between patients who will experience progression and those who will not within the training dataset. **(B)** The external validation results in this subfigure show insights into the model's ability to maintain discriminative performance in an independent validation dataset

relationship between vascular invasion and the survival prognosis of those with gastric carcinoma has been the focus of extensive scholarly inquiry, with numerous studies clarifying this association [18–20]. At the same time, the prognostic relevance of neural invasion has been established across various clinical populations, confirming it as a precursor to poor outcomes in gastric carcinoma [21]. This has led to its inclusion in specific clinical guidelines as a criterion for prescribing postoperative chemotherapy, enhancing early surgical interventions. However, despite the acknowledged link between neural invasion and unfavorable prognoses, predicting outcomes for patients with this condition is complicated by the variability of critical factors across different patient cohorts. The prognostic significance of "dual invasion"—the simultaneous occurrence of both vascular and neural invasions—is further complicated by the anatomical distribution of lymph node metastases and the extent of lymph node dissection techniques [22]. The presence of "dual invasion" may hasten the progression of the disease to a more advanced T stage, potentially adversely affecting patient prognoses [23]. This complex interplay calls for a nuanced understanding and careful consideration of these invasive characteristics in the context of personalized treatment planning for gastric carcinoma.

PTEN, a timeless guardian of cellular integrity, is often subdued in cancer [24]. Through its vigilant oversight, PTEN regulates many cellular processes, protecting against the invasive tendencies of wayward cells. It calms the reckless movements of cells by inhibiting the FAK pathway, suppresses the fiery aspirations of differentiation by moderating the MAPK pathway, and administers final judgment on cells by countering the seductive calls of the PI3K/Akt pathway [25–26]. Compared to its abundance in normal stomach mucosa, the limited presence of PTEN in dysplastic and cancerous tissues suggests its crucial role in the unfolding saga of gastric carcinogenesis [27]. Within the chaotic landscape of gastric cancer, classified into intestinal and diffuse types by histological experts [28], PTEN remains a beacon of distinction. It has been shown that PTEN's mournful presence dims in diffuse-type gastric cancer compared to its radiant shine in intestinal-type gastric cancer ($P < 0.05$) [27]. As a guardian of order, PTEN shapes cell destinies, influencing their adherence, differentiation, and mobility [29]. By curbing the reckless ambitions of Src/Stat3 and guiding cells toward a peaceful state, PTEN grants cancer cells the gift of anti-invasion [30]. When PTEN is restrained and its gaze averted, chaos follows as the fundamental polarity of cells is lost, leading them down a perilous path of dissemination [31]. The absence of PTEN's benevolent influence, coupled with an unfavorable microsatellite status, portends a grim future for those diagnosed with gastric cancer [32]. The whispers carried by miR-23a, concealed within the exosomes of gastric cancer cells, sow the seeds of angiogenic fervor by suppressing PTEN

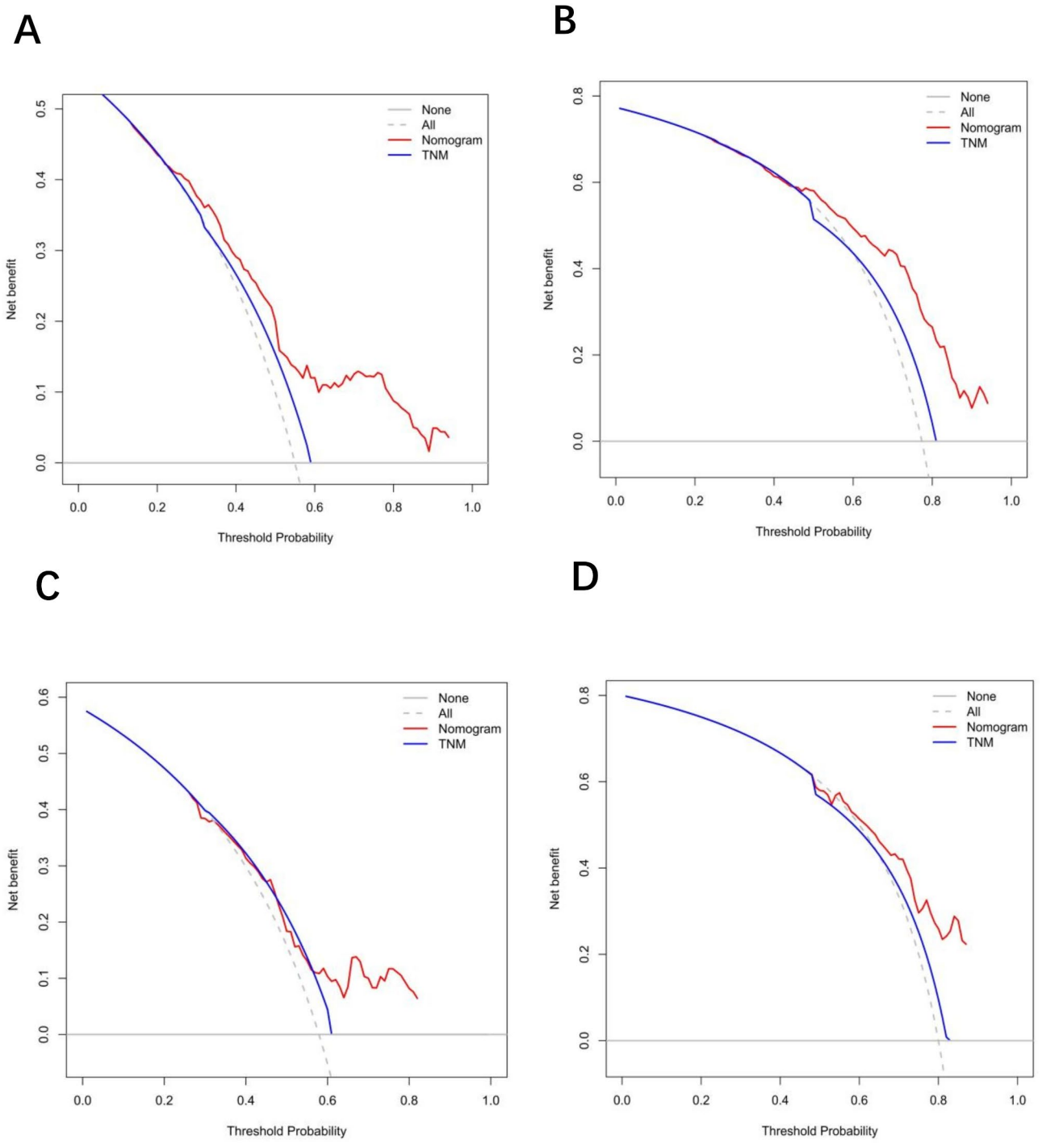

Fig. 7 Decision curve analysis (DCA) is employed to assess the clinical utility of the Lasso-cox regression model for predicting the 3-year and 5-year PFS of patients with "double invasion." **(A)** This subfigure presents the internal validation results for the 3-year PFS, demonstrating the model's potential net benefit across different threshold probabilities in the training cohort. **(B)** The external validation results for the 3-year PFS are shown in this subfigure, providing evidence of the model's clinical utility in an independent validation cohort. **(C)** Here, the internal validation for the 5-year PFS predictions is illustrated, offering insights into the long-term predictive value of the model within the training dataset. **(D)** This subfigure displays the external validation for the 5-year PFS, evaluating the model's clinical applicability and reliability in predicting long-term outcomes in a separate validation cohort

Table 3 NRI and IDI in the training set and the validation set

	Training cohort ($n=388$)		Validation cohort($n=171$)	
	8th AJCC TNM stage Vs Lasso-cox model	*P*	8th AJCC TNM stage Vs Lasso-cox model	*P*
NRI(95%CI)	0.218(0.08–0.343)	< 0.01	0.141(-0.108-0.373)	0.08
IDI(95%CI)	0.085(0.037–0.145	< 0.01	0.031(-0.036-0.113)	0.229

Abbreviations: CI, confidence interval; LASSO, least absolute shrinkage and selection operator; NRI, net reclassification improvement; IDI, integrated Discrimination Improvement Index; AJCC, American Joint Committee on Cancer

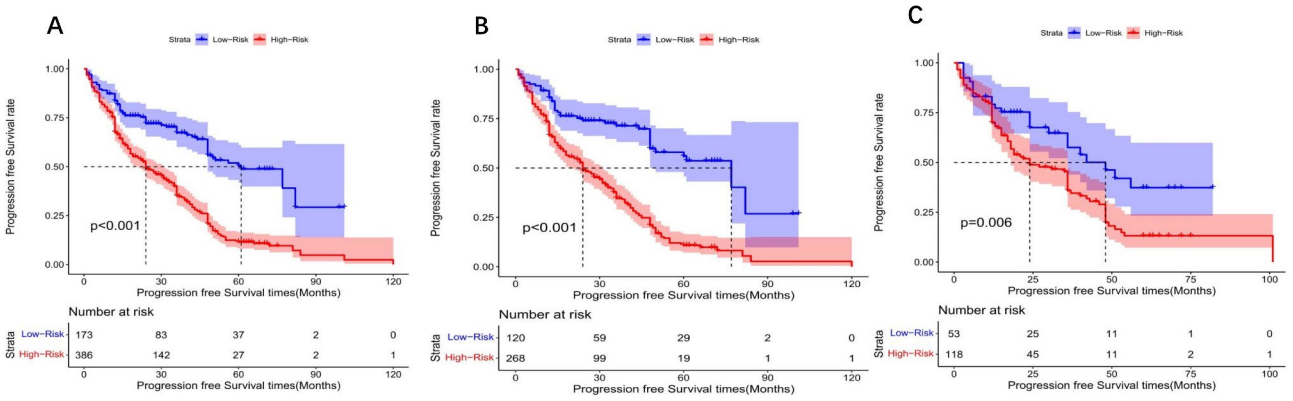

Fig. 8 Kaplan-Meier survival curves are used to visualize the survival outcomes of patients with varying "double invasion" scores across the overall, training, and validation cohorts. **(A)** This subfigure displays the survival curve for the entire cohort, including both the training and validation datasets, offering a comprehensive overview of survival outcomes linked to different levels of "double invasion." **(B)** The survival curve in this subfigure pertains specifically to the training cohort, emphasizing the survival differences among patients with varying "double invasion" scores within this subset of the data. **(C)** This subfigure concentrates on the validation cohort, illustrating the survival outcomes for patients with different "double invasion" scores in an independent dataset, thus validating the model's predictive capability

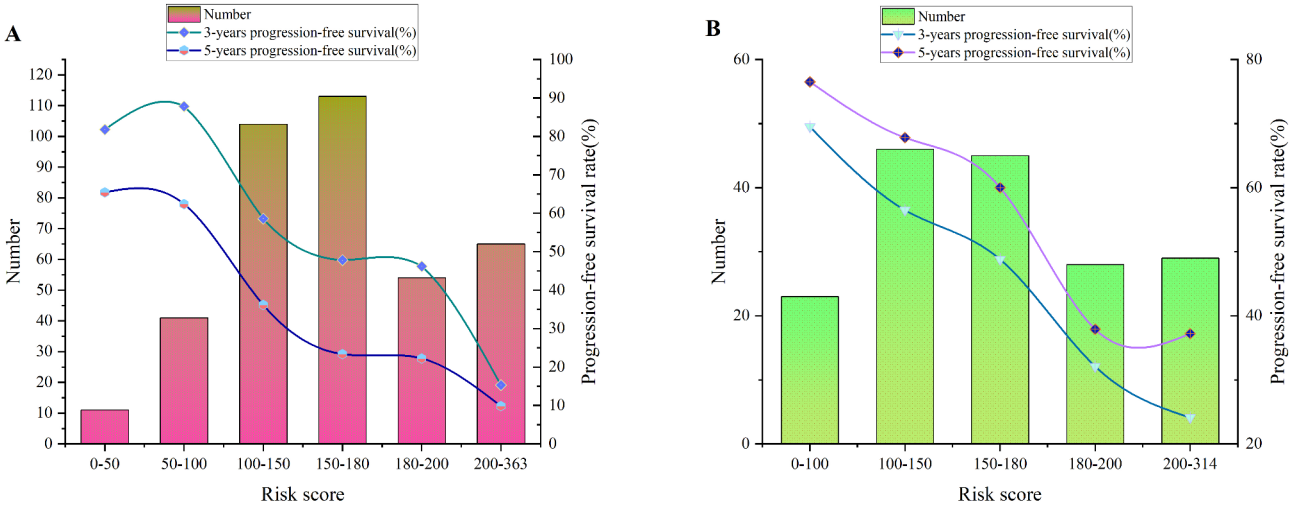

Fig. 9 The relationship between the risk score derived from the Lasso-cox regression model and the 3-year and 5-year PFS rates of patients is explored in this figure. **(A)** This subfigure displays the correlation between the risk score and the 3-year PFS rate within the training cohort, visually representing how the risk score relates to survival outcomes. **(B)** The external validation is presented in this subfigure, showing the correlation between the risk score and the 5-year PFS rate in the validation cohort, indicating the model's generalizability and reliability in predicting long-term survival outcomes

[33]. In response to this dire scenario, brave researchers have embarked on various quests, targeting specific nodes within the PTEN pathway in hopes of overcoming the forces of cancer [34]. Through the discerning lenses of Lasso and Cox regression, PTEN's presence emerges as a sign of hope for those involved in the tumultuous fight against gastric cancer. Its levels not only signify the stage of the disease but also reveal novel strategies for combating this formidable adversary.

The FHIT (fragile histidine triad), also known as human accelerated region 10, is situated at the delicate FRA3B on chromosome 3p14.2. Damage caused by carcinogens at this site can lead to gene translocations and abnormal transcripts. Spanning a vast 1.5 megabases, FHIT holds

the distinction of being the second-largest human gene. It encodes a 17kd diadenosine P1, P3-bis (5'-adenosyl)-triphosphate adenylohydrolase, playing a crucial role in purine metabolism. Functioning as a tumor suppressor, the FHIT protein can restrain cell proliferation and trigger apoptosis, independent of its hydrolase function [35]. By up-regulating the expression of thymidine kinase 1, FHIT causes an imbalance in dNTP levels and replication stress, resulting in various chromosomal abnormalities [36]. Additionally, FHIT is a crucial checkpoint in cell cycle regulation, engaging with activated tyrosine kinase receptors that recruit src [37]. Through phosphorylation at tyrosine 114 by src family tyrosine kinases, FHIT can induce apoptosis in lung cancer cells by reducing survivin expression and Akt activity [38]. Studies have revealed that decreased FHIT levels in gastric cancer are associated with aggressive behaviors and poor prognosis [39–41]. This study utilized FHIT protein expression as a potential marker for identifying gastric cancer patients with both vascular and neural invasion, highlighting its significance as a predictive indicator for those with "double invasion."

In exploring the labyrinth of gastric cancer, our immersive study meticulously analyzed the nuanced patient data in the face of this relentless malady. Over an extended period, we tracked the ebb and flow of their journeys, striving to unearth wisdom that could refine our therapeutic strategies and elevate the standard of care. We skillfully crafted a forest plot, intertwining lasso-Cox regression with a rich array of clinical, pathological, and molecular variables. This sophisticated graphical scheme emerged as a beacon, illuminating the survival landscape of patients confronted by "double invasion." It revealed a mosaic of influences, from the method of gastrectomy to the subtle molecular factors and the physical extent of the tumor—each an element in the complex brew of patient recovery. While earlier inquiries have utilized lasso-Cox regression for similar predictive efforts [42–47], rigorous internal and external validations emphasized our commitment to reliability, confirming the model's versatility and robustness across diverse clinical and patient demographics. The validation exercises yielded favorable outcomes, supporting our projections' accuracy, reliability, discriminative strength, and clinical utility. The model demonstrated its most pronounced predictive excellence over the 8th AJCC TNM stage classification within the training cohort. However, this superior performance was less evident when applied to the validation cohort. This discrepancy may arise from insufficient samples within the validation cohort. This endorsement further highlighted the enhanced prognostic precision and discriminative capabilities of lasso-Cox regression in the context of "double invasion." Going beyond validation, we undertook a population-based dissection to clarify the detailed risk stratification, enriching the predictive power of our forest plot. This strategy empowered clinicians to personalize treatment plans with greater insight and precision, improving the quality of care for those battling gastric cancer. Our holistic journey not only charts a more straightforward path for patient treatment but also equips healthcare practitioners with a powerful tool for informed decision-making. By merging the complexities of gastric cancer with the precision of predictive analytics, our effort aims to raise the standard of patient care and brighten the outlook for those facing this challenging disease.

Cytokeratin 20 (CK20) is a member of the cytokeratin family that exhibits a limited expression pattern in normal tissues. CK20 expression is a highly sensitive tumor marker for gastric adenocarcinoma, even in instances of peritoneal recurrence [48–50]. Similarly, CD56, typically associated with natural killer cells, is also expressed by various other immune cells, including alpha beta T cells, gamma delta T cells, dendritic cells, and monocytes [51–52]. In gastric cancer, CD56 is a marker for natural killer cells and is associated with disease progression and metastases [53–54]. Utilizing Cox regression, CK20 and CD56 have been identified as predictors of progression-free survival in "double invasion," highlighting the need for further investigation into the relationship between their expression and the presence of vascular and neural invasion.

The guarded outlook for patients with adenocarcinoma may stem from a confluence of factors, including disruptions in acetylation-related gene networks, alterations in mitochondrial function [55], the propensity for tumor budding [56], perturbations in long non-coding RNAs (lncRNAs) associated with anoikis resistance [57], and chromosomal instability [58]. Within the landscape of intratumoral heterogeneity, a high-clonality subtype correlates with advanced patient age, mutations in the TP53 gene, an enrichment of C > G transitions, and a marked reduction in survival duration. Conversely, a low-clonality subtype is linked to younger age, mutations in ARID1A and BRCA2, and significantly improved survival prospects [59]. Additionally, the use of metformin has emerged as a promising therapeutic strategy, correlating with enhanced survival in diabetic patients with gastric adenocarcinoma [60].

We have crafted a predictive plot with an innate, nature-inspired elegance to enhance our prognostication and risk stratification model. This groundbreaking methodology outlines the varying degrees of risk faced by patients experiencing "dual invasion," paving the way for customized treatment plans. Our model is essential in identifying low-risk patients, potentially eliminating unnecessary interventions, and flagging high-risk individuals who might benefit from targeted

therapies, providing critical insights for informed clinical judgments.

While the current study offers valuable insights, it is imperative to recognize the intrinsic constraints that shape its findings. Our meticulously crafted and validated model was initially based on datasets sourced exclusively from three healthcare institutions. This narrow demographic breadth may compromise the universality of our conclusions, underscoring the need for extensive validation across a diverse array of medical centers to affirm the model's dependability. Moreover, the investigation did not delineate between patients in the nascent and advanced phases of gastric carcinoma. This omission could potentially influence the precision of the model's predictive capabilities throughout the disease's progression. It is also noteworthy that the tumor biomarkers assessed within the study—spanning AE1/AE3, CK20, CDX-2, SATB-2, SYN, CGA, CD56, MLH1, PMS2, Her-2, PTEN, FHIT, MSH2, and MSH6—were subject to qualitative rather than quantitative scrutiny. Lastly, the model's predictive prowess was most pronounced compared with the 8th AJCC TNM stage classification within the training cohort. Yet, this predictive performance was not as discernibly superior when applied to the validation cohort. Future endeavors should categorize patients by disease stage to ascertain the model's robustness and refine its predictive efficacy.

Conclusion

This investigation introduces an enhanced predictive model crafted through the Lasso-Cox regression technique for identifying high-risk gastric carcinoma patients presenting with "double invasion. "This innovative method has the potential to refine the accuracy of identifying patients at heightened risk, thereby paving the way for more tailored prophylactic and therapeutic strategies.

Abbreviations

PFS	Progression free survival
AE1/AE3	Pan Cytokeratin Monoclonal Antibody
CK7	Cytokeratin 7
CK20	Cytokeratin 20
CDX-2	Caudal related homeobox transcription factor 2
STAB-2	Stabilin 2
SYN	Synaptophysin
CGA	Chromogranin A
CD 56	Cluster of Differentiation 56
MLH 1	MutL homologous gene 1
PMS 2	Postmitotic segregation increased 2
MSH2	MutS homolog 2
MSH6	MutS homolog 6
AJCC	American Joint Committee on Cancer
DCA	Decision curve analysis
t-ROC	time-dependent receiver operating characteristic
AUC	Area under the curve
NRI	Net Reclassification Improvement Index
IDI	Integrated Discrimination Improvement Index
CI	Confidence interval

Supplementary Information

The online version contains supplementary material available at https://doi.org/10.1186/s12885-025-13810-z .

Supplementary Material 1

Supplementary Material 2

Acknowledgements

Special thanks were given to Suwen Ji and Chenjie Fan for proofreading the patient follow-up information.

Author contributions

Liwei Wang and Yifan Li wrote the main manuscript text, and Yu Chang and Wenqing Qu prepared Figs. 1, 2, 3, 4, 5, 6, 7, 8 and 9. All authors reviewed the manuscript.

Funding

Supported by the Science and Education Cultivation Fund of the National Cancer and Regional Medical center of Shanxi Provincial Cancer hospital (SD2023005), Shanxi Provincial Key Discipline Special Fund(No: 2025051).

Data availability

Data is provided within the manuscript or supplementary information files.

Declarations

Ethics approval and consent to participate

We consulted extensively with the Ethics Committee of Shanxi Cancer Hospital and granted ethical approval from the Ethics Committee of Shanxi Carcinoma Hospital(No:2022JC23). All methods were performed according to the relevant guidelines and regulations. All procedures performed in studies involving human participants were by the ethical standards of our institutional research committee. Additionally, informed consent was obtained from all patients involved, indicating that they had given voluntary and informed consent to participate in the study. Written informed consent was obtained from all the patients for publication and accompanying images [61].

Consent for publication

Not applicable.

Competing interests

The authors declare no competing interests.

Author details

[1]Hepatobiliary, Pancreatic and Gastrointestinal Surgery, Shanxi Hospital Affiliated to Carcinoma Hospital, Chinese Academy of Medical Sciences, Shanxi Province Carcinoma Hospital, Carcinoma Hospital Affiliated to Shanxi Medical University, 030013 Taiyuan, Shanxi, China

Received: 18 January 2025 / Accepted: 25 February 2025
Published online: 28 February 2025

References

1. Sung H, Ferlay J, Siegel RL, Laversanne M, et al. Global Cancer statistics 2020: GLOBOCAN estimates of incidence and mortality worldwide for 36 cancers in 185 countries. CA Cancer J Clin. 2021;71(3):209–49.
2. Ajani JA, Lee J, Sano T, et al. Gastric adenocarcinoma. Nat Rev Dis Primers. 2017;3:17036.
3. Bourke MJ, Neuhaus H, Bergman JJ. Endoscopic submucosal dissection: indications and application in Western endoscopy practice. Gastroenterology. 2018;154(7):1887–e19005.
4. Salati M, Orsi G, Smyth E, et al. Gastric cancer: translating novel concepts into clinical practice. Cancer Treat Rev. 2019;79:101889.
5. Karimi P, Islami F, Anandasabapathy S, et al. Gastric cancer: descriptive epidemiology, risk factors, screening, and prevention. Cancer Epidemiol Biomarkers Prev. 2014;23(5):700–13.

6. Biagioni A, Skalamera I, Peri S, et al. Update on gastric cancer treatments and gene therapies. Cancer Metastasis Rev. 2019;38(3):537–48.
7. Strong VE, Wu AW, Selby LV, et al. Differences in gastric cancer survival between the U.S. And China. J Surg Oncol. 2015;112(1):31–7.
8. Katai H, Ishikawa T, Akazawa K, et al. Five-year survival analysis of surgically resected gastric cancer cases in Japan: a retrospective study of more than 100,000 patients from the nationwide registry of the Japanese gastric Cancer association (2001–2007). Gastric Cancer. 2018;21(1):144–54.
9. Cong R, Xu R, Ming J, Zhu Z. Construction of a preoperative nomogram model for predicting perineural invasion in advanced gastric cancer. Front Med (Lausanne). 2024;11:1344982.
10. Zhu Z, Mao M, Song A, Gong H, Gu J, Dai Y, Feng F. Study on the diagnostic value of MDCT extramural vascular invasion in preoperative N staging of gastric cancer patients. BMC Med Imaging. 2024;24(1):20.
11. Ge HT, Chen JW, Wang LL, et al. Preoperative lymphovascular and perineural invasion prediction in gastric cancer using spectral computed tomography imaging and machine learning. World J Gastroenterol. 2024;30(6):542–55.
12. Uno H, Cai T, Pencina MJ, et al. On the C-statistics for evaluating overall adequacy of risk prediction procedures with censored survival data. Stat Med. 2011;30(10):1105–17.
13. Harrell FE Jr, Lee KL, Mark DB. Multivariable prognostic models: issues in developing models, evaluating assumptions and adequacy, and measuring and reducing errors. Stat Med. 1996;15(4):361–87.
14. Li Y, Zhang X. Prognostic nomograms for gastric carcinoma after surgery to assist decision-making for postoperative treatment with chemotherapy cycles < 9 or chemotherapy cycles ≥ 9. Front Surg. 2022;9:916483.
15. Li Y, Bai M, Gao Y. Prognostic nomograms for gastric carcinoma after D2 + total gastrectomy to assist decision-making for postoperative treatment: based on Lasso regression. World J Surg Oncol. 2023;21(1):207.
16. Qu W, Li L, Ma J, Li Y. Screening high-risk individuals for primary gastric carcinoma: evaluating overall survival probability score in the presence and absence of lymphatic metastasis post-gastrectomy. World J Surg Oncol. 2024;22(1):196.
17. Park SH, Sohn TS, Lee J, et al. Phase III trial to compare adjuvant chemotherapy with capecitabine and cisplatin versus concurrent chemoradiotherapy in gastric cancer: final report of the adjuvant chemoradiotherapy in stomach tumors trial, including survival and subset analyses. J Clin Oncol. 2015;33(28):3130–6.
18. Noh SH, Park SR, Yang HK, et al. Adjuvant capecitabine plus oxaliplatin for gastric cancer after D2 gastrectomy (CLASSIC): 5-year follow-up of an open-label, randomized phase 3 trial. Lancet Oncol. 2014;15(12):1389–96.
19. Imai Y, Kurata Y, Ichinose M. The impact of venous invasion on the postoperative recurrence of pT1-3N0cM0 gastric Cancer. J Pers Med. 2023;13(5):734.
20. Li X, Wang Y, Zhai Z, et al. Predicting response to immunotherapy in gastric cancer via assessing perineural invasion-mediated inflammation in tumor microenvironment. J Exp Clin Cancer Res. 2023;42(1):206.
21. Jia H, Li R, Liu Y, et al. Preoperative prediction of perineural invasion and prognosis in gastric Cancer based on machine learning through a Radiomics-Clinicopathological nomogram. Cancers (Basel). 2024;16(3):614.
22. Ünal E, Karcaaltincaba M. Venous invasion in gastric Cancer. AJR Am J Roentgenol. 2020;214(1):W67.
23. Matsuo K, Lee SW, Tanaka R, et al. T stage and venous invasion are crucial prognostic factors for the long-term survival of patients with remnant gastric cancer: a cohort study. World J Surg Oncol. 2021;19(1):291.
24. Alvarez-Nuñez F, Bussaglia E, Mauricio D, et al. PTEN promoter methylation in sporadic thyroid carcinomas. Thyroid. 2006;16(1):17–23.
25. Ciuffreda L, Di Sanza C, Cesta Incani U, et al. The mitogen-activated protein kinase (MAPK) cascade controls phosphatase and tensin homolog (PTEN) expression through multiple mechanisms. J Mol Med (Berl). 2012;90(6):667–79.
26. Waite KA, Eng C. Protean PTEN: form and function. Am J Hum Genet. 2002;70:829–44.
27. Yang L, Kuang LG, Zheng HC, et al. PTEN encoding product: a marker for tumorigenesis and progression of gastric carcinoma. World J Gastroenterol. 2003;9(1):35–9.
28. Galon J, Mlecnik B, Bindea G, et al. Towards the introduction of the 'immunoscore' in the classification of malignant tumors. J Pathol. 2014;232(2):199–209.
29. Xu WT, Yang Z, Lu NH. Roles of PTEN (Phosphatase and tensin Homolog) in gastric cancer development and progression. Asian Pac J Cancer Prev. 2014;15(1):17–24.
30. Mukhopadhyay UK, Mooney P, Jia L, et al. Doubles game: Src-Stat3 versus p53-PTEN in cellular migration and invasion. Mol Cell Biol. 2010;30(21):4980–95.
31. Cavazzoni A, La Monica S, Alfieri R, et al. Enhanced efficacy of AKT and FAK kinase combined Inhibition in squamous cell lung carcinomas with stable reduction in PTEN. Oncotarget. 2017;8(32):53068–83.
32. Fan JP, Qian J, Zhao YJ. The loss of PTEN expression and microsatellite stability (MSS) were predictors of unfavorable prognosis in gastric cancer (GC). Neoplasma. 2020;67(6):1359–66.
33. Du J, Liang Y, Li J, et al. Gastric Cancer Cell-Derived Exosomal microRNA-23a promotes angiogenesis by targeting PTEN. Front Oncol. 2020 Mar;13:10:326.
34. Ertay A, Ewing RM, Wang Y. Synthetic lethal approaches to target cancers with loss of PTEN function. Genes Dis. 2023;10(6):2511–27.
35. Waters CE, Saldivar JC, Hosseini SA, et al. The FHIT gene product: tumor suppressor and genome caretaker. Cell Mol Life Sci. 2014;71(23):4577–87.
36. Karras JR, Schrock MS, Batar B, et al. Fhit loss-associated initiation and progression of neoplasia in vitro. Cancer Sci. 2016;107(11):1590–8.
37. Bianchi F, Magnifico A, Olgiati C, et al. FHIT-proteasome degradation caused by mitogenic stimulation of the EGF receptor family in cancer cells. Proc Natl Acad Sci U S A. 2006;103(50):18981–6.
38. Semba S, Trapasso F, Fabbri M, et al. Fhit modulation of the Akt-survivin pathway in lung cancer cells: Fhit-tyrosine 114 (Y114) is essential. Oncogene. 2006;25(20):2860–72.
39. Zheng HC, Liu LL. FHIT down-regulation was inversely linked to aggressive behaviors and adverse prognosis of gastric cancer: a meta- and bioinformatics analysis. Oncotarget. 2017;8(64):108261–73.
40. Czyzewska J, Guzińska-Ustymowicz K, Pryczynicz A, et al. Immunohistochemical assessment of Fhit protein expression in advanced gastric carcinomas correlates with Helicobacter pylori infection and survival time. Folia Histochem Cytobiol. 2009;47(1):47–53.
41. Zheng H, Takahashi H, Murai Y, et al. Low expression of FHIT and PTEN correlates with malignancy of gastric carcinomas: tissue-array findings. Appl Immunohistochem Mol Morphol. 2007;15(4):432–40.
42. Li H, Yang B, Wang C, et al. Construction of an interpretable model for predicting survival outcomes in patients with middle to advanced hepatocellular carcinoma (≥ 5 cm) using lasso-cox regression. Front Pharmacol. 2024;15:1452201.
43. Li P, Zhang Q, Zhang Q, et al. A LASSO Cox regression predictive model for patients undergoing surgery for pancreatic body and tail adenocarcinoma patients: comparative Long-Term survival analysis of radical antegrade modular pancreatosplenectomy (RAMPS) and standard retrograde pancreatosplenectomy (SPRS). Ann Surg Oncol. 2024;31(12):8317–26.
44. Chen J, Yu F, He G, et al. A nomogram based on peripheral lymphocyte for predicting 8-year survival in patients with prostate cancer: a single-center study using LASSO-cox regression. BMC Cancer. 2024;24(1):254.
45. Luo B, Yang M, Han Z, et al. Establishment of a Nomogram-Based prognostic model (LASSO-COX Regression) for predicting Progression-Free survival of primary Non-Small cell lung Cancer patients treated with adjuvant Chinese herbal medicines therapy: A retrospective study of case series. Front Oncol. 2022;12:882278.
46. Wang W, Liu W. Integration of gene interaction information into a reweighted Lasso-Cox model for accurate survival prediction. Bioinformatics. 2021;36(22–23):5405–14.
47. Chu J, Sun N, Hu W, et al. Bayesian hierarchical Lasso Cox model: A 9-gene prognostic signature for overall survival in gastric cancer in an Asian population. PLoS ONE. 2022;17(4):e0266805.
48. Altree-Tacha D, Tyrrell J, Haas T. CDH17 is a more sensitive marker for gastric adenocarcinoma than CK20 and CDX2. Arch Pathol Lab Med. 2017;141(1):144–50.
49. Takata A, Kurokawa Y, Fujiwara Y, et al. Prognostic value of CEA and CK20 mRNA in the peritoneal lavage fluid of patients undergoing curative surgery for gastric cancer. World J Surg. 2014;38(5):1107–11.
50. Satoh Y, Mori K, Kitano K, et al. Analysis for the combination expression of CK20, FABP1, and MUC2 is sensitive for the prediction of peritoneal recurrence in gastric cancer. Jpn J Clin Oncol. 2012;42(2):148–52.
51. Rodriguez-Mogeda C, van Ansenwoude CMJ, van der Molen L, et al. The role of CD56bright NK cells in neurodegenerative disorders. J Neuroinflammation. 2024;21(1):48.
52. Van Acker HH, Capsomidis A, Smits EL, et al. CD56 in the immune system: more than a marker for cytotoxicity?? Front Immunol. 2017;8:892.

53. Peng LS, Mao FY, Zhao YL, et al. Altered phenotypic and functional characteristics of CD3 + CD56 + NKT-like cells in human gastric cancer. Oncotarget. 2016;7(34):55222–30.
54. Izawa S, Kono K, Mimura K H_2O_2 production within tumor microenvironment inversely correlated with infiltration of CD56(dim) NK cells in gastric and esophageal cancer: possible mechanisms of NK cell dysfunction. Cancer Immunol Immunother., Xing W, Yi N et al. Comprehensive analysis of acetylation-related.
55. gene sets and mitochondrial functions in gastric adenocarcinoma: implications for prognosis and therapeutic strategies. Front Immunol. 2024;15:1451725.
56. Kemi N, Eskuri M, Ikäläinen J, et al. Tumor budding and prognosis in gastric adenocarcinoma. Am J Surg Pathol. 2019;43(2):229–34.
57. Li Q, Zhang H, Hu J, et al. Construction of anoikis-related LncRNAs risk model: predicts prognosis and immunotherapy response for gastric adenocarcinoma patients. Front Pharmacol. 2023;14:1124262.
58. Silva ANS, Saito Y, Yoshikawa T, et al. Increasing frequency of gene copy number aberrations is associated with immunosuppression and predicts poor prognosis in gastric adenocarcinoma. Br J Surg. 2022;109(3):291–7.
59. Chen K, Yang D, Li X, et al. Mutational landscape of gastric adenocarcinoma in Chinese: implications for prognosis and therapy. Proc Natl Acad Sci U S A. 2015;112(4):1107–12.
60. Zheng J, Santoni G, Xie SH, et al. Improved prognosis in gastric adenocarcinoma among Metformin users in a population-based study. Br J Cancer. 2021;125(2):277–83.
61. Wang J, Li Y, Liang S. Screening high-risk individuals for primary gastric adenocarcinoma: evaluating progression-free survival probability score in the presence and absence of rictor expression after gastrectomy. Front Oncol. 2024;14:1382818.

Publisher's note